

Electrogenerated Chemiluminescence. 66. The Role of Direct Coreactant Oxidation in the Ruthenium Tris(2,2')bipyridyl/Tripropylamine System and the Effect of Halide Ions on the Emission Intensity

Yanbing Zu and Allen J. Bard*

Department of Chemistry and Biochemistry, The University of Texas at Austin, Austin, Texas 78712

We describe the electrogenerated chemiluminescence (ECL) processes of the Ru(bpy)₃²⁺ (bpy = 2,2'-bipyridyl)/tripropylamine (TPrA) system at glassy carbon, platinum, and gold electrodes. The electrochemical behavior of TPrA on different electrode materials and its influence on the ECL process are demonstrated. At glassy carbon electrodes, the direct oxidation of TPrA began at ~0.6 V vs SCE and exhibited a broad irreversible anodic peak. Two ECL waves were observed, one in the potential region more negative than 1.0 V vs SCE and one at more positive potentials. The first ECL process apparently occurs without the electrogeneration of Ru(bpy)₃³⁺, in contrast to that of the second ECL wave. At Pt and Au electrodes, however, the formation of surface oxides significantly blocked the direct oxidation of TPrA. An ECL wave below 1.0 V did not appear at Pt and was very weak at gold. The ECL peaks at potentials of 1.1–1.2 V were also much weaker than those observed at the glassy carbon electrode. These results showed that the direct oxidation of TPrA played an important role in the ECL processes. Therefore, the enhancement of the TPrA oxidation current might lead to an increase in the ECL intensity. Small amounts of halide species were found to inhibit the growth of surface oxides on Pt and gold electrodes and led to an obvious increase of TPrA oxidation current. The anodic dissolution of gold in halide-containing solution was also important in activating the gold electrode surface. The electrochemical catalytic effect of bromide further promoted the oxidation of TPrA. A halide effect on ECL at Pt and Au electrodes was also evident. The most effective enhancement of ECL was observed at Au electrode in a bromide-containing solution. This effect was also found in a commercial flow-through instrument (IGEN) and provided a simple way to improve the detection sensitivity at low concentrations of Ru(bpy)₃²⁺.

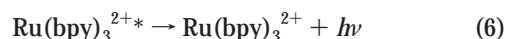
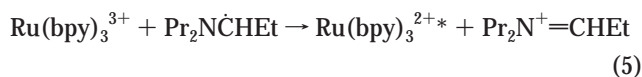
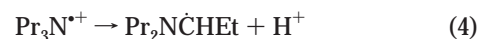
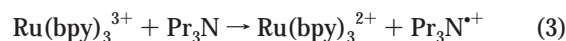
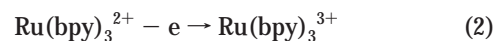
We address in this paper the effect of direct oxidation of a coreactant at an electrode on the ECL emission intensity. In the classical ECL experiments, excited states are produced by electron transfer between oxidized (R⁺) and reduced (R⁻) species gener-

ated at an electrode by alternating potential steps or sweeps or at closely spaced pairs of electrodes:¹



For R = Ru(bpy)₃²⁺ (bpy = 2,2'-bipyridyl), the redox reaction, e.g., in MeCN, occurs between Ru(bpy)₃³⁺ and Ru(bpy)₃²⁺.² In analytical ECL systems, however, emission can be generated by a potential sweep or step in a single direction by the addition of a coreactant that produces one of the reactants.³ For example, when tri-*n*-propylamine (TPrA or Pr₃N) is used as coreactant with the Ru(bpy)₃²⁺ system,⁴ the reactions can be expressed by

Scheme 1



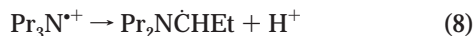
(where Pr = CH₃CH₂CH₂- and Et = CH₃CH₂-)

The excited state in this scheme is generated by reaction 5 where the highly reducing radical species, Pr₂N $\dot{\text{C}}$ HEt, reacts with Ru(bpy)₃³⁺. In this path, called the catalytic or EC' route, the oxidation of TPrA occurs by reaction with electrogenerated Ru(bpy)₃³⁺. Under some conditions the oxidation of TPrA can occur

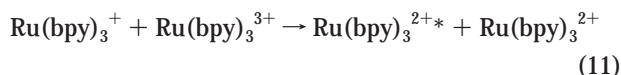
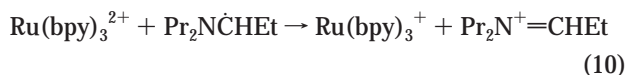
- (1) For review of ECL, see: (a) Faulkner, L. R.; Bard, A. J. In *Electroanalytical Chemistry*; Bard, A. J., Ed.; Marcel Dekker: New York, 1977; Vol. 10, p 1. (b) Knight A. W.; Greenway, G. M. *Analyst* **1994**, *119*, 879.
- (2) Tokel-Takvoryan, N.; Hemingway, R.; Bard, A. J. *J. Am. Chem. Soc.* **1973**, *95*, 6582.
- (3) (a) Rubinstein, I.; Bard, A. J. *J. Am. Chem. Soc.* **1981**, *103*, 512. (b) White, H. S.; Bard, A. J. *J. Am. Chem. Soc.* **1982**, *104*, 6891. (c) Ege, D.; Becker, W. G.; Bard, A. J. *Anal. Chem.* **1984**, *56*, 2413.
- (4) (a) Noffsinger, J. B.; Danielson, N. D. *Anal. Chem.* **1987**, *59*, 865. (b) Leland, J. K.; Powell, M. J. *J. Electrochem. Soc.* **1990**, *137*, 3127.

directly at the electrode:

Scheme 2



In both routes, reaction of the radical with $\text{Ru}(\text{bpy})_3^{2+}$ can also occur:



(In the following text, $\text{Pr}_3\text{N}^{\bullet+}$ and $\text{Pr}_2\text{N}\dot{\text{C}}\text{HEt}$ will be presented as $\text{TPrA}^{\bullet+}$ and TPrA^{\bullet} , respectively.)

The relative contributions of the two routes to formation of excited states and observed emission depends on the electrode potential, the relative concentrations of $\text{Ru}(\text{bpy})_3^{2+}$ and TPrA , the rate of the homogeneous reaction 3, and factors that affect the potential and rate of oxidation of TPrA at the electrode. For example, in a previous study,^{4b} the initial rise in ECL was assigned to the catalytic route, but the direct oxidation route became more important at more positive potentials.

The anodic reactions of aliphatic amines in aprotic and aqueous solutions have been investigated at various electrodes.⁵ Previous studies showed that the oxidation of TPrA at a platinum electrode in acetonitrile solution exhibits an anodic peak at ~ 0.8 V vs SCE.^{5a} The anodic behavior of some tertiary amines at a glassy carbon electrode has also been examined in aqueous alkaline solutions.^{5b,e} In aqueous $\text{Ru}(\text{bpy})_3^{2+}$ ECL analysis, the optimum pH value of the TPrA buffer solution is usually about 7–8, and concentrated TPrA (around 100 mM) is usually used to achieve high ECL intensity.^{4b}

An understanding of the mechanism of the $\text{Ru}(\text{bpy})_3^{2+}/\text{TPrA}$ system is important in improving the sensitivity and reproducibility of ECL systems, such as those that utilize $\text{Ru}(\text{bpy})_3^{2+}$ as a label in immunoassays and DNA probes.⁶ In this paper, the ECL processes of the $\text{Ru}(\text{bpy})_3^{2+}/\text{TPrA}$ system at different electrodes are examined, and the importance of the direct oxidation of TPrA is demonstrated. Details of the kinetics and mechanism of the $\text{Ru}(\text{bpy})_3^{2+}/\text{TPrA}$ system will be reported elsewhere.⁷ TPrA oxidation at Pt and gold electrodes is shown to be promoted by a small amount of halide species, and consequently, the ECL intensity can be increased significantly.

(5) (a) Mann, C. K. *Anal. Chem.* **1964**, *36*, 2424. (b) Masui, M.; Sayo, H.; Tsuda, Y. *J. Chem. Soc. B* **1968**, 973. (c) Portis, L. C.; Mann, C. K. *J. Org. Chem.* **1970**, *35*, 2175. (d) Ross, S. D. *Tetrahedron Lett.* **1973**, *15*, 1237. (e) Smith, J. R. L.; Masheder, D. *J. Chem. Soc., Perkin Trans. 2* **1976**, 47.

(6) (a) Blackburn, G. F.; Shah, H. P.; Kenten, J. H.; Leland, J.; Kamin, R. A.; Link, J.; Peterman, J.; Powell, M. J.; Shah, A.; Talley, D. B.; Tyagi, S. K.; Wilkins, E.; Wu, T. G.; Massey, R. J. *Clin. Chem.* **1991**, *37*, 1534. (b) Bard, A. J.; Whitesides, G. U.S. Patent 5,238,808, 1993. (c) Xu, X.-H.; Bard, A. J. *J. Am. Chem. Soc.* **1995**, *117*, 2627.

(7) Kanoufi, F.; Zu, Y.; Bard, A. J., in preparation.

EXPERIMENTAL SECTION

Chemicals were used as received. $\text{Ru}(\text{bpy})_3\text{Cl}_2 \cdot 6\text{H}_2\text{O}$ (minimum 98%) was obtained from Strem Chemicals (Newburyport, MA). Tripropylamine (99+%) from Aldrich (Milwaukee, WI) was dissolved in 0.15 M phosphate buffer solution (PBS). The pH value of the solution was adjusted to 7.5 with concentrated NaOH or H_3PO_4 . All solutions were prepared with deionized water (Milli-Q, Millipore).

Cyclic voltammetry was carried out with the model 660 electrochemical workstation (CH Instruments, Austin, TX). Glassy carbon (GC), platinum, and gold electrodes were polished with 0.05- μm alumina to obtain a mirror surface and then were ultrasonicated and thoroughly rinsed with Milli-Q water. The reference electrode was a saturated calomel electrode (SCE). A coiled platinum wire was used as the auxiliary electrode. For experiments in the conventional electrochemical cell, all solutions are deaerated with N_2 and a constant flow of N_2 was maintained over the solution during the measurements. Before each experiment, the electrode was subjected to repeated cycling in the potential region of -0.7 V to $+1.4$ V (vs SCE) in 0.15 M PBS until a reproducible voltammogram was obtained. The ECL signal was measured with a photomultiplier tube (PMT, Hamamatsu R4220p) installed under the electrochemical cell. A voltage of 750 V was supplied to the PMT with a high-voltage power supply series 225 (Bertan High Voltage Corp., Hicksville, NY). The current density and the normalized ECL intensity (PMT output, I_{ECL}) were calculated according to the geometrical surface area of the electrodes.

A charge-coupled device (CCD) camera (Photometrics CH260) cooled to below -135 °C interfaced to a personal computer was used to obtain ECL spectra. The camera was focused on the output of a grating spectrometer (Holographics, Inc., concave grating and 1-mm entrance slit). The CCD camera and general configuration of the spectra acquisition have been described previously.⁸

The flow-through system was an Origen I analyzer (IGEN Inc., Gaithersburg, MD). This instrument integrates a photometer, potentiostat, electrochemical cell, and flow injection system for fluid and sample handling. The working and counter electrodes in the IGEN cell were gold disks with equal areas of 0.71 cm^2 . The reference electrode, Ag/AgCl, was ~ 5 cm downstream of the working electrode and detector. The solution for cleaning the cell and the buffer for bringing the samples contained 0.02% (in volume) Triton X-100. These solutions were not deaerated. All experiments were carried out at room temperature.

RESULTS AND DISCUSSION

Electrochemistry and ECL Reactions of the $\text{Ru}(\text{bpy})_3^{2+}/\text{TPrA}$ System. *Glassy Carbon Electrode.* Figure 1a shows the cyclic voltammograms (CV) of a GC electrode in 0.15 M PBS (pH 7.5). In the absence of $\text{Ru}(\text{bpy})_3^{2+}$ and TPrA , a scan between 0 and $+1.4$ V vs SCE is featureless, with the current increase beginning at $\sim +1.25$ V signaling the onset of electrode surface oxidation. Studies on the electrochemical behavior of GC electrodes in contact with aqueous solutions have shown that, compared to metal or other carbon electrodes, such as various graphites, GC

(8) McCord, P.; Bard, A. J. *J. Electroanal. Chem.* **1991**, *318*, 91.

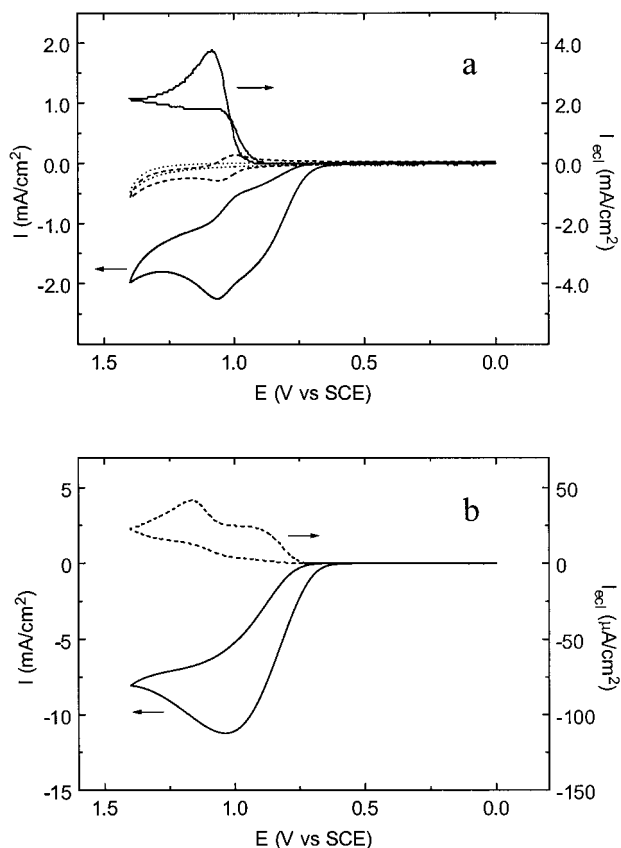


Figure 1. (a) Cyclic voltammograms of 1 mM $\text{Ru}(\text{bpy})_3^{2+}$ at a glassy carbon electrode in 0.15 M phosphate buffer solution (pH 7.5) in the presence (solid line) and absence (dashed line) of 10 mM TPrA. The dotted line represents data in the absence of both $\text{Ru}(\text{bpy})_3^{2+}$ and TPrA. The ECL signal curve was recorded during the CV in buffer solution containing 1 mM $\text{Ru}(\text{bpy})_3^{2+}$ and 10 mM TPrA. (b) Cyclic voltammogram and ECL curve at a glassy carbon electrode in 0.15 M phosphate buffer solution (pH 7.5) containing 100 mM TPrA and 1 μM $\text{Ru}(\text{bpy})_3^{2+}$. Potential scan rate, 0.1 V/s.

exhibits greater inertness to chemical attack.⁹ At high concentrations of $\text{Ru}(\text{bpy})_3^{2+}$ (≥ 1 mM) the well-known reversible CV wave was observed with $E_p = 1.1$ V. Upon addition of 10 mM TPrA, its direct oxidation started at ~ 0.6 V, with the ECL emission occurring at the potentials of the $\text{Ru}(\text{bpy})_3^{2+}$ oxidation. With the addition of TPrA, the anodic wave for $\text{Ru}(\text{bpy})_3^{2+}$ oxidation is greatly enhanced and the reduction wave disappears, as expected for the EC' reaction scheme of eqs 2–6.

The behavior was different for very small concentrations of $\text{Ru}(\text{bpy})_3^{2+}$. When relatively concentrated TPrA (100 mM) was present in the PBS, a small amount of $\text{Ru}(\text{bpy})_3^{2+}$ could lead to obvious light emission, as shown in Figure 1b. The rather broad irreversible anodic wave was primarily due to the direct oxidation of TPrA, and 1 μM $\text{Ru}(\text{bpy})_3^{2+}$ had little influence on the CV. The oxidation current started to rise at ~ 0.6 V and its peak potential was ~ 1.1 V. This completely irreversible anodic oxidation behavior is similar to that of TPrA in acetonitrile solution on a Pt electrode^{5a} and in basic aqueous solution on a glassy carbon electrode.^{5b}

As shown in Figure 1b, two ECL waves appeared during the positive scan. The first one occurred at ~ 0.75 V and formed a

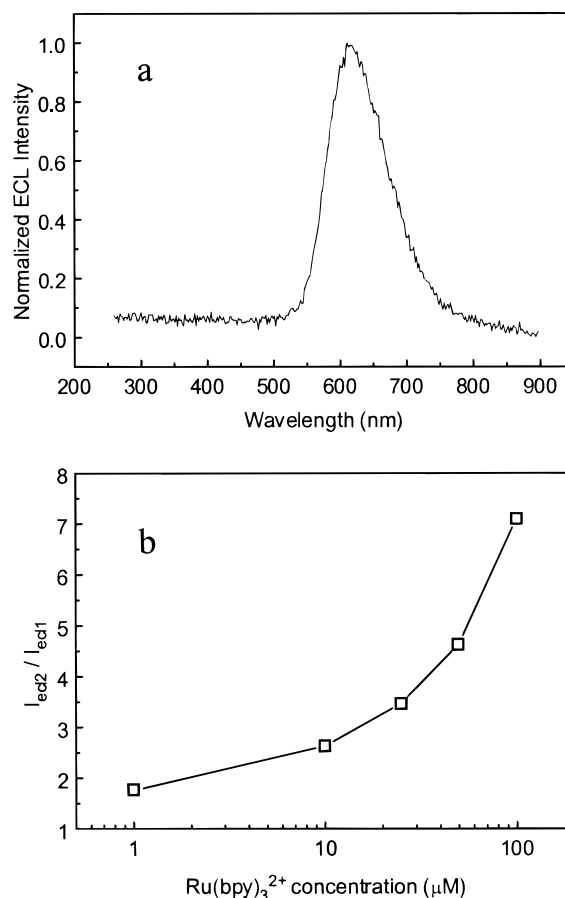


Figure 2. (a) Normalized spectrum of the first ECL wave at a glassy carbon electrode in 0.15 M phosphate buffer solution (pH 7.5) containing 100 mM TPrA and 1 μM $\text{Ru}(\text{bpy})_3^{2+}$. Electrode was held at 0.9 V vs SCE. (b) Dependence of the intensity ratio of the two ECL waves at a glassy carbon electrode on $\text{Ru}(\text{bpy})_3^{2+}$ concentration in 0.15 M phosphate buffer solution (pH 7.5) containing 10 mM TPrA. $I_{\text{ECL}1}$ represents the ECL intensity at 0.9 V. $I_{\text{ECL}2}$ represents the peak value of the second ECL wave.

plateau at 0.9 V. Beyond 1.0 V, the ECL intensity increased again, reaching its maximum at 1.2 V. The second ECL peak was consistent with that shown in Figure 1a and its mechanism can be described as Schemes 1 and 2. However, the intense ECL wave below 1.0 V has not been discussed in earlier studies. The spectrum of the ECL signal at 0.9 V is shown in Figure 2a, indicating that the light was the emission of $\text{Ru}(\text{bpy})_3^{2+*}$. The onset potential of the first ECL wave is too negative to generate appreciable amounts of $\text{Ru}(\text{bpy})_3^{3+}$ that could receive an electron from the highly reducing species (TPrA $^{\cdot}$) to form $\text{Ru}(\text{bpy})_3^{2+*}$. In addition, according to the ECL mechanism presented in Scheme 1, the nearly exponential increase of $\text{Ru}(\text{bpy})_3^{3+}$ concentration with potential would result in a rapid rise of ECL intensity rather than the constant plateau behavior observed between 0.9 and 1.0 V. These results suggest that the mechanism at the first ECL wave is different from that usually used to describe the ECL process (Schemes 1 and 2), because the electrogenerated $\text{Ru}(\text{bpy})_3^{3+}$ species cannot play a significant role in this ECL route. Because the direct oxidation of TPrA leads to the formation of reducing radicals (TPrA $^{\cdot}$) that could react with $\text{Ru}(\text{bpy})_3^{2+}$ to generate $\text{Ru}(\text{bpy})_3^{3+}$ (eq 10), one possible way to produce $\text{Ru}(\text{bpy})_3^{2+*}$ could be the electron transfer from $\text{Ru}(\text{bpy})_3^{3+}$ to some

(9) (a) McCreery, R. L. In *Electroanalytical Chemistry*; Bard, A. J., Ed.; Marcel Dekker: New York, 1992; Vol. 17. (b) Vanderlinden, W. E.; Dieker, J. W. *Anal. Chim. Acta* **1980**, *119*, 1.

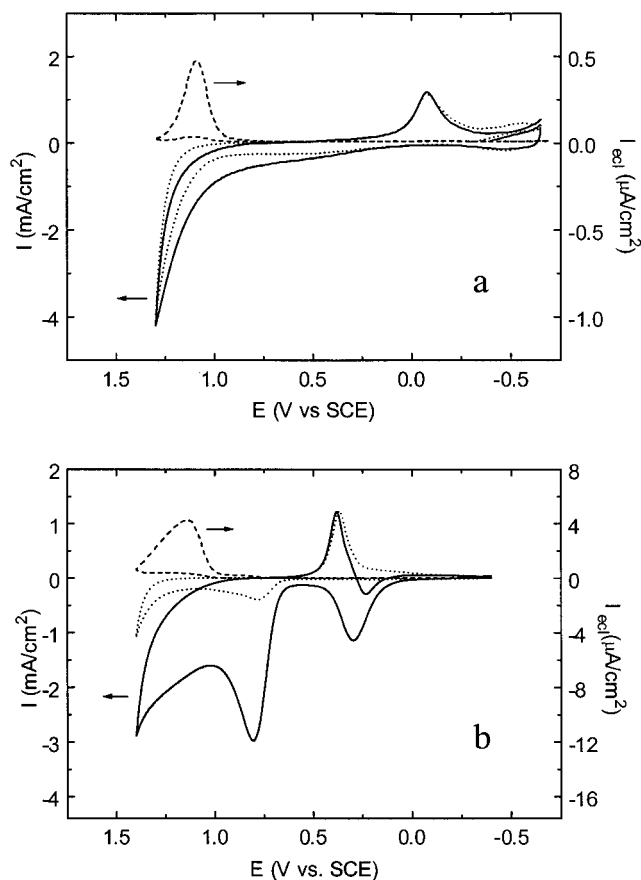


Figure 3. Cyclic voltammogram and ECL curve at (a) platinum and (b) gold electrodes in 0.15 M phosphate buffer solutions (pH 7.5) containing 100 mM TPrA and 1 μ M Ru(bpy) $_3^{2+}$. The dotted line represents data in the absence of both Ru(bpy) $_3^{2+}$ and TPrA. Potential scan rate, 0.1 V/s.

oxidative species. It is unlikely that the radical cation of TPrA, which undergoes a very rapid deprotonation reaction, could be the oxidant, and other likely candidates are not apparent. The Ru(bpy) $_3^+$ could be oxidized at the electrode itself, although one would think that Ru(bpy) $_3^{2+}$ formed right at the electrode surface would be quenched by the electrode quite efficiently.

The intensity of the first ECL wave leveled off before the TPrA oxidation current reached its maximum value. A further increase of ECL intensity beyond 1.0 V occurred in the region of electro-generation of Ru(bpy) $_3^{3+}$, which followed the usual ECL reaction routes to emit light. The first ECL wave was comparable in intensity to the second one. As the concentration of Ru(bpy) $_3^{2+}$ increased, however, the relative intensity of the second ECL wave became larger and larger, as shown in Figure 2b. Thus, at Ru(bpy) $_3^{2+}$ concentrations above \sim 0.5 mM, the homogeneous catalytic reaction between TPrA and electrogenerated Ru(bpy) $_3^{3+}$ plays the dominant role in the ECL process.

Platinum Electrode. Figure 3a shows the CVs at a platinum electrode in the PBS in the absence and presence of 100 mM TPrA. The ECL curve was obtained when 1 μ M Ru(bpy) $_3^{2+}$ was present in the PBS containing 100 mM TPrA. The electrochemical oxidation of the platinum surface (i.e., formation of adsorbed OH and O species) began at \sim 0.2 V during the positive scan, and TPrA oxidation also occurred in this region. However, the oxidation current of TPrA was quite small below 1.0 V. As the

electrode potential became more positive, a rapid rise of the anodic current was observed, which can be attributed mainly to the oxidation of H $_2$ O. Compared to the CV at a GC electrode, TPrA oxidation started at a much more negative potential on Pt, but the current was much lower until the region of water oxidation.

The growth of anodic oxide films at noble metals has been extensively studied.^{10,11} The primary reaction in this process is an electrochemical discharge step that proceeds as a fast under-potential deposition reaction. Fractional coverage by electrode-deposited species such as OH and O is established rapidly at any given potential. Following the initial deposition of a submonolayer, a two-dimensional array of OH and O species and an oxide film at the monolayer level form. The presence of surface oxides can have a variety of effects on the reaction of an electroactive species. For some redox reactions, the oxides exhibit a catalytic effect at low coverage.¹² The appearance of the oxidation current of TPrA following the deposition of O-containing species at much more negative potential than 0.6 V suggested that these surface species were able to catalyze the oxidation of TPrA, although this catalytic reaction rate was quite low. The oxidation current increased very slowly even after the electrode potential was scanned beyond 0.6 V, where a much larger anodic current commenced at a GC electrode. This indicated that the surface oxide seriously inhibited the direct oxidation of TPrA.

At the platinum electrode, only one ECL peak at \sim 1.1 V was observed. Since direct TPrA oxidation was inhibited by the surface oxide, the highly reducing radical (TPA \cdot) was not generated effectively by the direct oxidation of TPrA in the lower potential region, and the first ECL process observed at the GC electrode was not seen at the platinum electrode. When the electrode potential was scanned positively beyond 0.9 V, upon the oxidation of Ru(bpy) $_3^{2+}$, an ECL signal was observed and its intensity increased rapidly. This ECL process was of the same nature as that of the second ECL wave at the GC electrode. Both direct and catalytic oxidation of TPrA were involved in the ECL reactions. However, due to the much lower direct oxidation rate of TPrA at Pt electrodes, the contribution of the route described in Scheme 2 to the ECL was much smaller. This resulted in a normalized ECL intensity at Pt \sim 100 times lower than at GC.

Gold Electrode. Figure 3b shows the CVs at a gold electrode in the PBS. In the absence of TPrA, the growth of surface oxide began at \sim 0.65 V. In the solution containing 0.1 M TPrA, two anodic peaks appeared at 0.3 and 0.8 V. The first peak extended between about 0.1 and 0.5 V. In the reverse scan, following the reduction of surface oxide, the oxidation current appeared again. The surface processes of the gold electrode in the so-called double-layer potential region are not clear, and there is significant confusion in the literature with regard to behavior in this region.^{10a,11} Extra charge over that needed to electrostatically charge the double layer in this potential region has been observed.

(10) (a) Woods, R. In *Electroanalytical Chemistry*; Bard, A. J., Ed.; Marcel Dekker: New York, 1977; Vol. 9. (b) Conway, B. E.; Barnett, B.; Angerstein-Kozłowska, H. *J. Chem. Phys.* **1990**, *93*, 8361.

(11) (a) Angerstein-Kozłowska, H.; Conway, B. E.; Hamelin, A.; Stoicovicu, L. *J. Electroanal. Chem.* **1987**, *228*, 429. (b) Burke, L. D.; Lyons, M. E. G. In *Modern Aspects of Electrochemistry*; White, R. E., Bockris, J. O'M., Conway, B. E., Eds.; Plenum Publishing Corp.: New York, 1986; Vol. 18, p 169 and references therein.

(12) (a) Davis, D. G. *Talanta* **1960**, *3*, 335. (b) Muller, L.; Nekrassov, L. N. *J. Electroanal. Chem.* **1965**, *9*, 282. (c) Muller, L. *J. Electroanal. Chem.* **1968**, *16*, 531.

The origin of this pseudocapacitance was suggested to be the specific adsorption of the anions with full or almost full charge transfer.^{11a} Some authors proposed that premonolayer oxidation may occur at the gold electrode.^{11b} The active metal adatoms can be oxidized at potentials well below that required to initiate regular monolayer oxide (or OH_{ad}) formation. The product was assumed to be low coverage (or incipient) hydrous oxide species that mediate oxidation processes at the electrode surface. In our experiments, the small anodic current peak at low potential might result from a catalytic effect of the adsorbed species on TPrA oxidation.

When the electrode potential was scanned beyond 0.6 V, the direct oxidation process of TPrA started. This occurs in the same potential region where the surface oxide grows. The oxide coverage increased rapidly and led to the formation of a complete oxide monolayer. The anodic current dropped after 0.8 V. Since the peak current density was much smaller than that observed at the GC electrode, the decrease of the TPrA oxidation rate can be attributed to passivation of the gold surface in this potential region, rather than diffusion control. In the potential region more positive than 1.0 V, the TPrA oxidation current increased gradually.

At the gold electrode in a 1 μM Ru(bpy)₃²⁺ and 100 mM TPrA solution, a very weak ECL emission was observed below 1.0 V, while the main ECL peak appeared at 1.15 V (Figure 3b). The normalized ECL peak intensity was ~10 times higher than that at the Pt electrode and ~10 times lower than that at the GC electrode.

The above experiments clearly show that the electrode material has a significant effect on the ECL process in the Ru(bpy)₃²⁺/TPrA system, which would not be expected for the purely catalytic route, eqs 2–6. This can mainly be attributed to the importance of the direct oxidation of TPrA in the emission process and the strong effect of electrode surface condition on this electrode reaction. In the potential region below 1.0 V, where no appreciable amount of Ru(bpy)₃³⁺ was generated, the direct oxidation of TPrA results in an ECL signal by generating Ru(bpy)₃^{2+*} via an unknown mechanism. Note that at all electrodes the background ECL from TPrA oxidation in the absence of Ru(bpy)₃²⁺ was at least 100 times smaller than that seen with 1 μM Ru(bpy)₃²⁺. At the GC electrode, the large TPrA oxidation current gave rise to an intense first ECL wave. The formation of surface oxides at the gold and platinum electrodes, however, inhibits the direct oxidation of TPrA, so that the first ECL wave was much weaker at gold and almost disappeared on Pt.

At these electrodes, the main ECL peaks appeared beyond 1.0 V and their intensities also obviously depended on the direct oxidation rate of TPrA. Since the catalytic oxidation of TPrA by electrogenerated Ru(bpy)₂³⁺ occurs slowly in dilute (micromolar) Ru(bpy)₂²⁺ solutions, the contribution of this route to the formation of excited states is relatively less important than that of the direct oxidation of TPrA. Therefore, the most intense ECL was observed at the GC electrode, while the ECL intensity at the gold and platinum electrodes was about 10 and 100 times lower, respectively.

In addition, because Pt is a good catalyst for water decomposition, the rapid increase in anodic current for the oxidation of water and the evolution of O₂, which can produce quenchers of Ru(bpy)₂^{2+*}, was observed in the CV beyond 1.0 V. The decom-

position of H₂O also resulted in the decrease of pH value near the electrode surface, leading to a further decrease of ECL intensity.⁴ The ECL peak potential was less positive at a Pt electrode, and the ECL signal dropped more rapidly with Pt than that at the other electrodes. For example, at 1.25 V, the ECL signal almost disappeared completely on Pt while it was still obvious on GC and gold. The rate of H₂O decomposition was much lower at the GC and gold electrodes below 1.4 V and had less influence on the ECL reactions than at the platinum electrode.

Halide Effect. The above results suggested that the ECL intensity could be enhanced for low Ru(bpy)₃²⁺ concentrations by increasing the direct TPrA oxidation rate at the electrode. Since a lower rate of the direct oxidation of TPrA at platinum and gold electrodes resulted from coverage by surface oxides, inhibiting or retarding the growth of these oxides should promote the oxidation of TPrA. The adsorption of halide at platinum and gold electrodes, which can retard the formation of surface oxides, has been extensively studied.^{13–16} Chemisorbed halide layers that withstand rinsing with water and electrolyte solution can form irreversibly at the electrode surface with the adsorption strength decreasing in the sequence I⁻ > Br⁻ > Cl⁻. Aqueous I⁻ is reported to react with the electrode surface to form an uncharged adsorbed species, whereas Br⁻ and Cl⁻ are adsorbed in anionic form.^{15,16} Halide anion may also be present in a reversible adsorbed state. We examined the effect of these halide species on the anodic oxidation of TPrA, which led to a pronounced enhancement of the oxidation current as well as an increase in the ECL intensity in the presence of Ru(bpy)₃²⁺ in most cases.

Platinum Electrode. Studies on the adsorption of iodide and iodine at Pt and Au electrodes have led to the conclusion that aqueous iodide undergoes oxidative chemisorption to form a close-packed layer of zerovalent iodine at the electrode surface.^{15,16} Figure 4a shows that, in the PBS containing 0.1 mM iodide, the formation of Pt surface oxide moved to more positive potentials by ~0.5 V. An anodic peak appeared at ~0.75 V due to the oxidation of adsorbed iodine to iodate (IO₃⁻) which accompanied the oxidation of the Pt surface. This I⁻ effect is in agreement with that reported by others in acidic solutions.^{15,16a} The oxidation of TPrA in the potential region of 0.2–0.6 V was suppressed by the adsorbed iodine layer. The chemisorbed iodine obviously blocked the deposition of surface species that could catalyze TPrA oxidation in the low-potential region. When the electrode potential was scanned positive beyond 0.6 V, the oxidation current started to increase rapidly and an anodic peak formed at ~0.75 V. This anodic peak involved the oxidative desorption of chemisorbed iodine, formation of electrode surface oxide, and oxidation of TPrA. By comparison with the CVs in Figure 4a in the absence of TPrA, the peak current was mainly attributed to the last reaction. When the anodic oxidation of TPrA started at ~0.6 V, the electrode surface was covered by an iodine layer. The I-coated electrode was reported to be only slightly less conductive than the I-free surface and the electron-transfer reaction between the electrode

(13) (a) Breiter, M. W. *Electrochim. Acta* **1963**, *8*, 925. (b) Bold, W.; Breiter, M. W. *Electrochim. Acta* **1961**, *5*, 145.

(14) Novak, D. M.; Conway, B. E. *J. Chem. Soc., Faraday Trans.* **1981**, *77*, 2341.

(15) Lane, R. F.; Hubbard, A. T. *J. Phys. Chem.* **1975**, *79*, 808.

(16) (a) Rodriguez, J. F.; Harris, J. E.; Bothwell, M. E.; Mebrahtu, T.; Soriaga, M. P. *Inorg. Chim. Acta* **1988**, *148*, 123. (b) Berry, G. M.; Bothwell, M. E.; Bravo, B. G.; Cali, G. J.; Mebrahtu, T.; Michelhaugh, S. L.; Rodriguez, J. F.; Soriaga, M. P. *Langmuir* **1989**, *5*, 707.

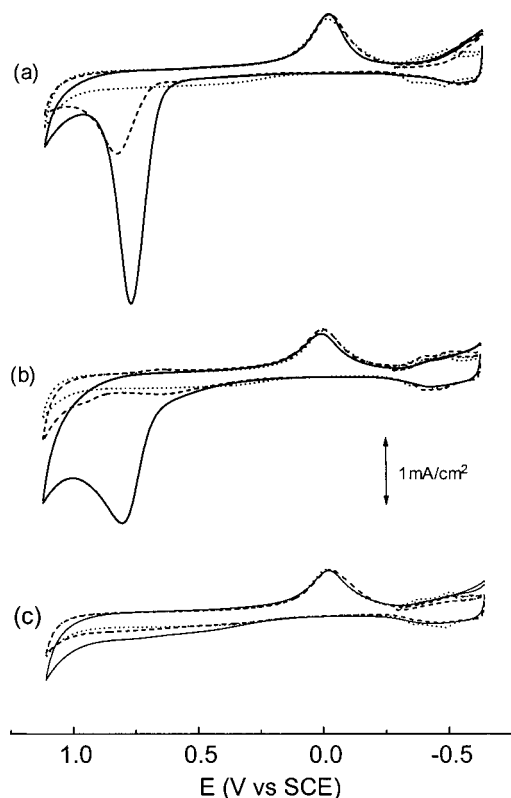


Figure 4. Cyclic voltammograms of 100 mM TPrA at a platinum electrode in 0.15 M phosphate buffer solution (pH 7.5) containing (a) 0.2 mM iodide, (b) 1 mM bromide, and (c) 1 mM chloride (solid lines). The dashed lines represent the data in the absence of TPrA. The dotted lines represent the data in the absence of both TPrA and halide ions. Potential scan rate, 0.1 V/s.

and aqueous species is not blocked by this layer.^{16b} Therefore, the I-coated Pt surface was much more active for TPrA oxidation than the Pt oxide-covered surface. During the desorption of the chemisorbed iodine, the formation of surface oxide occurred immediately, and the electrode became inert rapidly, resulting in a sharp drop of the anodic current.

Figure 4b shows similar results for bromide at the Pt electrode. The adsorbed Br⁻ also obviously blocked the initial stage of the surface oxide growth. A small anodic current peak for Br⁻ oxidation was observed at ~0.9 V, and consequently, the reduction current of the products of Br⁻ oxidation appeared at ~0.65 V in the reverse scan. Besides bromine, bromate species could also be formed upon oxidation of Br⁻ in the neutral buffer solution.^{17a} Obvious enhancement of TPrA oxidation in the potential region more positive than 0.6 V was observed in the bromide-containing solution. The electrochemical catalytic oxidation of TPrA by bromine was involved in the anodic peak, since during the reverse scan in the presence of TPrA, the reduction wave of the products of bromide oxidation disappeared completely. Primary, secondary, and tertiary amines have been reported to be oxidatively cleaved by aqueous bromine at room temperature.^{18,19} Therefore, in the present experiments, the electrogenerated bromine can oxidize

(17) (a) Kelsall, G. H.; Welham, N. J.; Diaz, M. A. *J. Electroanal. Chem.* **1993**, *361*, 13. (b) Diaz, M. A.; Kelsall, G. H.; Welham, N. J. *J. Electroanal. Chem.* **1993**, *361*, 25.

(18) Deno, N. C.; Fruit, R. E. *J. Am. Chem. Soc.* **1968**, *90*, 3502.

(19) Bellucci, G.; Bianchini, R. *J. Chem. Soc., Perkin Trans. 2* **1987**, 39.

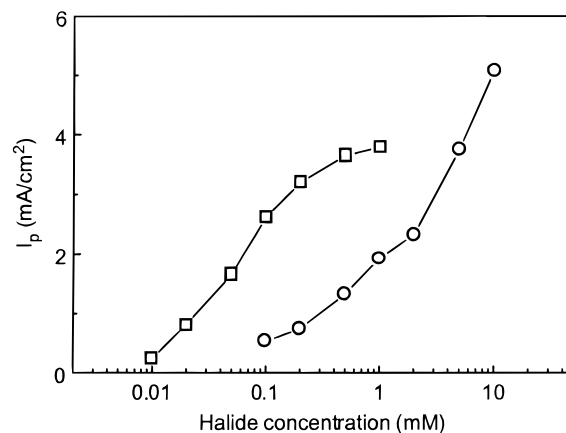
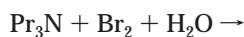


Figure 5. Dependence of oxidation peak current (I_p) of 100 mM TPrA at a platinum electrode on the concentration of iodide (□) and bromide (○) in the phosphate buffer solution (pH 7.5). Potential scan rate, 0.1 V/s.

TPrA in the overall reaction



The oxidation peak in Figure 4a was much narrower than that in Figure 4b. This might be caused by the narrower potential range of the adsorption of iodide compared to bromide. In addition, the catalytic oxidation of TPrA by electrogenerated bromine might also contribute to the relatively larger oxidation current of TPrA at potentials above 1.0 V.

Figure 4c shows that the adsorbed chloride ions exhibited a much weaker blocking effect on the growth of Pt surface oxide in neutral solution, although the effect is evident in a previous study in acidic solution.¹⁴ The weak adsorption of chloride does not shift the formation of the inert surface oxide monolayer appreciably. On the other hand, the adsorption of Cl⁻ suppressed the slight catalytic effect of the surface O-containing species, resulting in a slight decrease of TPrA oxidation current.

In summary, at a Pt electrode, the electrochemical deposition of O and OH occurred at a quite low potential. Adsorbed I⁻ and Br⁻ species retarded the growth of surface oxides and promoted the anodic oxidation of TPrA. However, Cl⁻ showed little effect on either surface oxide growth or TPrA oxidation due to its much weaker adsorption. Figure 5 shows the dependence of the oxidation peak current of TPrA on the concentration of halide ions in solution. At low concentration, I⁻ was more effective than Br⁻. This is consistent with the known fact that I⁻ is more strongly adsorbed at noble metal surfaces. The higher current obtained at relatively concentrated Br⁻ solution was attributed partially to the catalytic oxidation of TPrA by electrogenerated bromine.

Because a small amount of iodide and bromide species obviously promoted TPrA oxidation, an increase in the ECL of the Ru(bpy)₃²⁺/TPrA system was also observed in the halide-containing solutions, as shown in Figure 6. The enhancement of TPrA oxidation current led to the appearance of an ECL peak or shoulder at ~0.85 V. This ECL signal should have the same nature as the first wave observed at the GC electrode in Figure 1b. Because of its stronger adsorption, iodide exhibited a greater effect

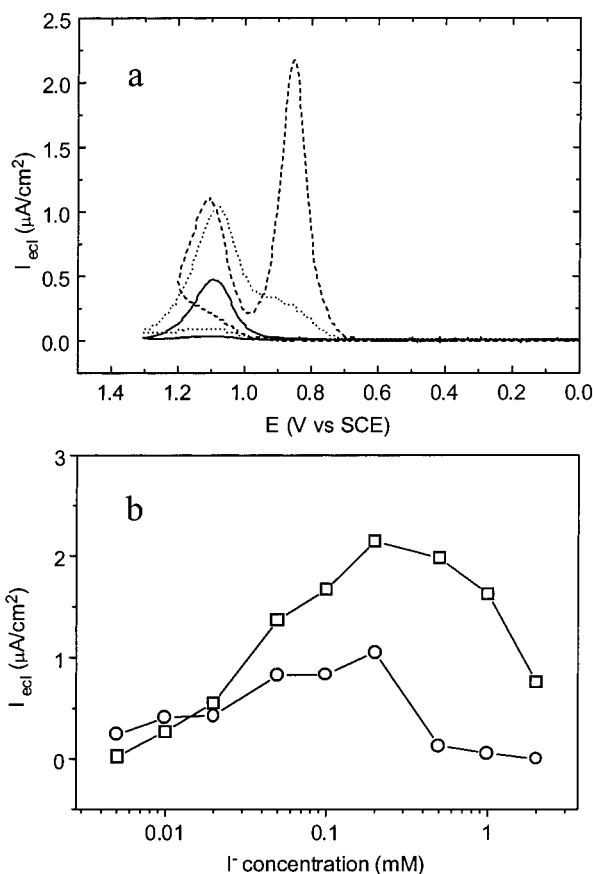


Figure 6. (a) ECL curves at a Pt electrode in $1 \mu\text{M Ru}(\text{bpy})_3^{2+}$, 100 mM TPrA , and $0.15 \text{ M phosphate buffer solution (pH 7.5)}$ in the absence (solid line) and presence of 0.2 mM iodide (dashed line) or 1 mM bromide (dotted line). (b). Dependence of the intensity of the first ECL peak (\square) and the second ECL peak (\circ) at a Pt electrode on the concentration of iodide. Potential scan rate, 0.1 V/s .

than bromide. The ECL peak at $\sim 1.1 \text{ V}$ was also increased in the presence of I^- and Br^- .

Figure 6b shows the dependence of the two ECL peaks on iodide concentration. Upon addition of a small amount of iodide, the first ECL peak rose more rapidly and became higher than the second one. The increase of the ECL intensity was consistent with the rise of the direct TPrA oxidation current. However, when iodide concentration became larger than 0.2 mM , the intensities of both ECL peaks dropped, although no decrease of the TPrA oxidation current was seen (Figure 5). A similar dependence of ECL on bromide concentration was also observed. At higher concentrations of iodide and bromide, oxidation products can destroy the highly reducing radical species (TPrA^*), leading to a decrease of ECL intensity. Moreover these species are quenchers of $\text{Ru}(\text{bpy})_3^{2+*$ (See Figures S1 and S2 in Supporting Information). Therefore, high concentrations of halide ions decrease the ECL emission.

Little effect on ECL intensity was observed upon the addition of chloride ions in the $\text{Ru}(\text{bpy})_3^{2+}/\text{TPrA}$ system. This was consistent with the result of the small effect of chloride on the oxidation of TPrA at Pt electrodes.

In the above solutions, the electrogenerated $\text{Ru}(\text{bpy})_3^{3+}$ may also be reduced by the halide species. However, due to the much lower reaction constants (k) of these processes (for Cl^- , Br^- , and I^- , k has been determined to be $<2 \times 10^{-3}$, 50 , and $1 \times 10^5 \text{ M}^{-1}$

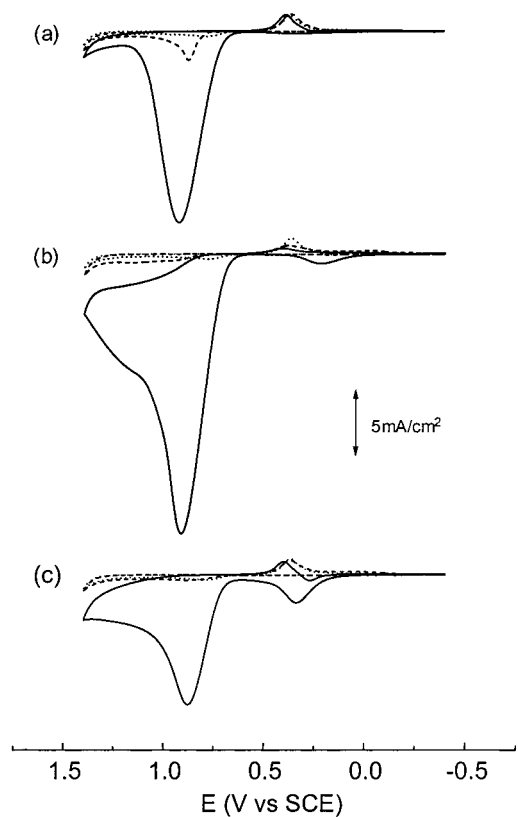


Figure 7. Cyclic voltammograms of 100 mM TPrA at a gold electrode in $0.15 \text{ M phosphate buffer solution (pH 7.5)}$ containing (a) 0.1 mM iodide , (b) 1 mM bromide , and (c) 1 mM chloride . The dotted lines represent the data in the absence of both TPrA and halide ions. Potential scan rate, 0.1 V/s .

s^{-1} , respectively)²⁰ compared to that of reaction 3 ($\sim 1.3 \times 10^7 \text{ M}^{-1} \text{ s}^{-1}$)⁷ and the much lower concentration of halide ions compared to that of TPrA, the consumption of $\text{Ru}(\text{bpy})_3^{3+}$ by these routes should be negligible.

Gold Electrode. Halide species can also adsorb either irreversibly or reversibly on a gold electrode. In addition, halides anions are stable complexants for soluble gold species.¹⁷ Thus, in the positive potential region, the dissolution of a gold electrode is enhanced by aqueous halide ions.²¹ The thermodynamics of different Au–halide– H_2O systems have been summarized recently.¹⁷

The electrochemical behavior of iodide at a gold electrode is shown in Figure 7a. The onset of gold surface oxide was at $\sim 0.65 \text{ V}$ in the PBS in the absence of halide species, i.e., at more positive potentials than at a Pt electrode. The adsorbed iodine species blocked the initial stage of surface oxide formation. An anodic peak due to the oxidation of the adsorbed iodine layer appeared at 0.87 V . Compared to Figure 4a, the oxidative desorption of iodine occurred at a more positive potential, which suggests that the Au– $\text{I}_{(\text{ad})}$ bond is more stable than the Pt– $\text{I}_{(\text{ad})}$ bond.

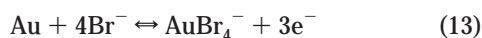
Figure 7a also shows the effect of chemisorbed iodine on the oxidation of TPrA at the gold electrode. The iodine layer

(20) Rabini, J.; Hashimoto, K.; Liu, Z. F.; Fujishima, A. *Langmuir* **1993**, *9*, 818.

(21) (a) Gaur, J. N.; Schmid, G. M. *J. Electroanal. Chem.* **1970**, *24*, 279. (b) Frankenthal, R. P.; Siconolfi, D. J. *J. Electrochem. Soc.* **1982**, *129*, 1192. (c) Honbo, H.; Sugawara, S.; Itaya, K. *Anal. Chem.* **1990**, *62*, 2424. (d) Ye, S.; Ishibashi, C.; Shimazu, K.; Uosaki, K. *J. Electrochem. Soc.* **1998**, *145*, 1614. (e) Ye, S.; Ishibashi, C.; Shimazu, K.; Uosaki, K. *Langmuir* **1999**, *15*, 807.

suppressed the first anodic process in the potential region between 0.1 and 0.5 V. The strong chemisorption of iodine inhibited the adsorption of OH⁻ or other surface-oxidized species that might catalyze TPrA oxidation. The second oxidation process starting at ~0.6 V, however, was significantly promoted by the adsorbed iodine layer. After reaching its maximum at 0.92 V, the anodic current dropped sharply. This effect of chemisorbed iodine was similar to that observed at a Pt electrode (See Figure 4a). The retardation of the formation of the inert oxide monolayer on a gold electrode led to the enhancement of the TPrA oxidation current. Since the desorption of iodine layer on gold was more difficult than on Pt, the growth of surface oxide initiated at more positive potential at the gold electrode in iodide-containing solution, which resulted in the larger anodic peak current of TPrA oxidation in Figure 7a than that in Figure 4a. After the desorption of iodine layer and the formation of a surface oxide monolayer, the TPrA oxidation current became quite small.

Figure 7b shows that the adsorbed Br⁻ also delayed the formation of surface oxide. As the Br⁻ concentration increased, a rise in the anodic current in the potential region more positive than 0.8 V was seen. In this potential region, bromide could be oxidized. Another important anodic process was the dissolution of the gold electrode. In the presence of bromide ions, the gold dissolved predominantly in the form of the tetrabromo complex.^{17a,21a}



E (V vs SHE) =

$$0.854 + 0.0789 \log[\text{Br}^-] - 0.0148 \log[\text{AuBr}_4^-]$$

The first oxidation peak of TPrA between 0.1 and 0.5 V became higher upon the addition of a small amount of Br⁻ in the solution and then was inhibited when Br⁻ was more concentrated. This probably results from the competitive influence of bromide on the adsorption of oxidizing surface species and Au oxidation. As the electrode potential became more positive than 0.6 V, the second oxidation peak of TPrA was significantly increased by bromide. When Br⁻ was more concentrated than 0.5 mM, a current shoulder appeared following the oxidation peak. Increasing the Br⁻ concentration further led to a slight suppression of the anodic peak current (see Figure 8). At potentials more positive than 0.8 V, the oxidation of Br⁻ occurred and the catalytic oxidation of TPrA by the electrogenerated Br₂ (eq 12) participated in the anodic processes. Previous studies^{17,21} showed that, due to the enhanced dissolution of gold in solutions containing Br⁻ or Cl⁻, the passivation of the gold electrode surface became more difficult. This was probably another important contribution to the high TPrA oxidation current. In relatively concentrated bromide solutions, the evolution of Br₂ and the formation of Br₃⁻, was significant. The presence of Br₂ and Br₃⁻ can also inhibit the discharge of bromide at anode surface sites.²² These species probably also suppressed TPrA oxidation and led to the decrease of the anodic peak current, as shown in Figure 8.

Figure 7c shows that chloride ions also exhibited a slight blocking effect on the initial stage of gold surface oxide growth,

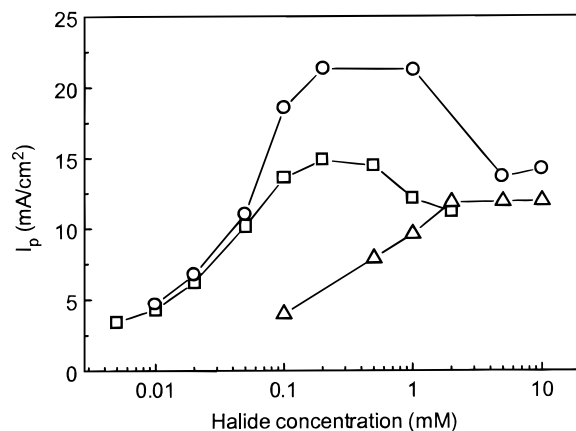
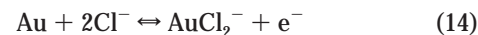


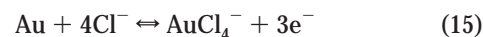
Figure 8. Dependence of oxidation peak current (I_p) of 100 mM TPrA at a gold electrode on the concentration of iodide (□), bromide (○), and chloride (△) in the phosphate buffer solution (pH 7.5). Potential scan rate, 0.1 V/s.

although its adsorption was weaker than that of I⁻ and Br⁻. In addition, studies of Au anode behavior in solutions containing Cl⁻ have shown that the anodic dissolution of gold was evident.^{17,21}



E (V vs SHE) =

$$0.910 + 0.05916 \log[\text{AuCl}_2^-] - 0.11832 \log[\text{Cl}^-]$$



E (V vs SHE) =

$$0.764 + 0.0197 \log[\text{AuCl}_4^-] - 0.0788 \log[\text{Cl}^-]$$

The dissolution rate of gold was proportional to the Cl⁻ concentration and the potential for the passivation of gold shifted positively.^{17,21}

In solutions containing Cl⁻, both the first and the second TPrA oxidation peaks became higher. In relatively concentrated chloride solution, the second oxidation peak became broader. Because of the strong enhancement of gold dissolution and the delay of the passivation of electrode surface in the chloride-containing solution, the chance for the direct oxidation of TPrA at an oxide-free gold site was significantly increased. The depassivating effect of chloride ions on gold is also the basis for the leaching of gold in chloride media.^{17a}

At a gold electrode, I⁻, Br⁻, and Cl⁻ all exhibited a significant positive effect on the oxidation of TPrA. Because the first oxidation process at a gold electrode is much less important compared to the anodic reaction proceeding at a higher potential, either from the point of view of its slower rate or of the ECL application, our attention mainly focused on the second oxidation process. Figure 8 shows the dependence of peak current of the second TPrA oxidation process on the concentration of halide ion in the PBS solutions. Bromide exhibited the most significant effect in enhancing the TPrA oxidation current. Although the adsorption of chloride on gold was much weaker than that of iodide and bromide, which resulted in an insensitivity of TPrA oxidation on the addition of a small amount of chloride (<0.1 mM), relatively

(22) Conway, B. E.; Phillips, Y.; Qian, S. Y. *J. Chem. Soc., Faraday Trans.* **1995**, *91*, 283.

concentrated chloride solutions promoted the dissolution of gold and, consequently, enhanced the TPrA oxidation current. Figure 8 also shows that, when adequate amounts of halide ions were present in the solution, the peak current of TPrA oxidation at the gold electrode was higher than that at the GC electrode in the PBS (see Figure 1b).

Pt is usually a better catalyst for the oxidation of organic species in acidic or neutral media. However, the above results suggested a smaller activity of Pt compared to gold for the oxidation of TPrA. This is mainly because the growth of surface oxide was much easier at a Pt surface, and once covered by a compact oxide monolayer, the catalytic effect of a Pt electrode was significantly inhibited. Comparison between Figures 5 and 8 shows that the halide effect was generally more important at Au than at Pt. The stronger adsorption of halide species at a gold surface as well as the enhancement of gold dissolution in concentrated halide solution more effectively postponed the passivation of the electrode, which resulted in the greater rise of TPrA oxidation current.

Consistent with the enhancement of TPrA oxidation current, there was a significant halide effect on the ECL in the $\text{Ru}(\text{bpy})_3^{2+}$ /TPrA system at a gold electrode, as shown in Figure 9a. In solutions containing iodide, an increase in the first ECL peak was greatest. The resulting broad ECL peak extended to ~ 1.2 V. In the potential region more positive than 1.0 V, the TPrA oxidation current was quite low (See Figure 7a), so the ECL intensity was weaker than that in solutions containing bromide or chloride. Bromide and chloride exhibited a greater effect on the second ECL peak than on the first. Figure 9b shows the dependence of the intensities of the two ECL waves on bromide concentration. As discussed above, relatively concentrated halide ion suppressed the ECL signals. The strongest ECL signal was observed in a solution containing 0.1 mM bromide. Compared to that in the halide-free solution, the ECL intensity was almost 100 times higher; even compared to that at the GC electrode, an ECL intensity ~ 10 times greater was achieved.

The influence of halide ions on the ECL reaction of the $\text{Ru}(\text{bpy})_3^{2+}$ /TPrA system at GC electrodes was also studied. No obvious effect was observed when dilute halide ions were present, while relatively concentrated iodide and bromide species resulted in a decrease in the ECL intensity. This is consistent with the ready oxidation of TPrA on GC and the quenching effects at higher concentrations.

Effect of Bromide in the Flow Injection System. In the commercial ECL system, a flow injection approach is used. The bromide effect was examined in an IGEN flow cell in the Origen instrument with gold as the working electrode. Figure 10a shows the dependence of ECL intensity of 1 nM $\text{Ru}(\text{bpy})_3^{2+}$ on bromide concentration in the PBS containing 50 mM TPrA. The most intense ECL signal was obtained when 1 mM bromide was present. This value was larger than that shown in Figure 9b. In the flow system, to avoid the entrapment of gas bubbles, surfactant (Triton X-100) is added to the PBS to reduce the solution surface tension. The competition between the adsorption of surfactant species and bromide ions on the working electrode surface would suppress the bromide effect and the optimum bromide concentration became higher. When the TPrA concentration was lower, a smaller optimum bromide concentration was found (Figure 10b).

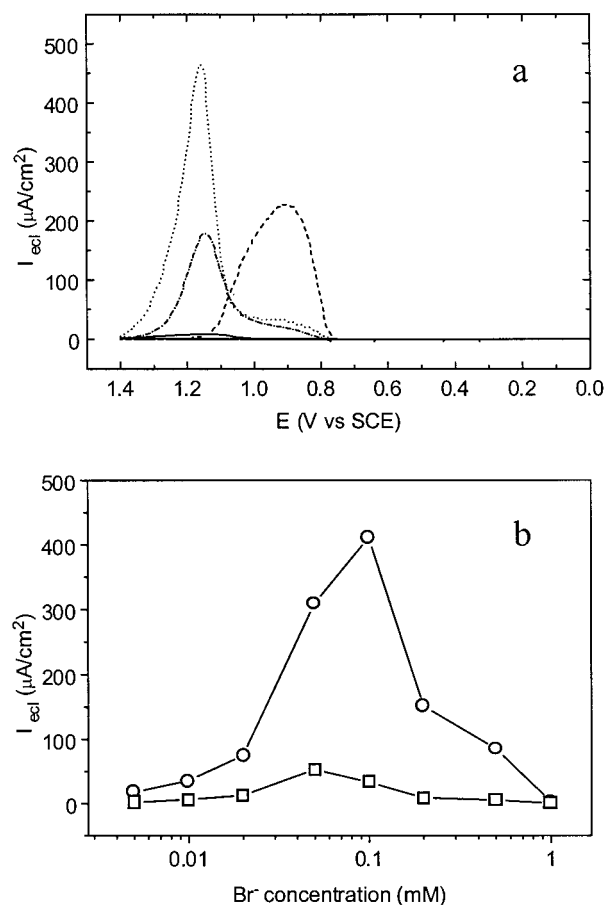


Figure 9. (a) ECL curves at a gold electrode in 1 μM $\text{Ru}(\text{bpy})_3^{2+}$, 100 mM TPrA, and 0.15 M phosphate buffer solution (pH 7.5) in the absence (solid line) and presence of 0.1 mM iodide (dashed line), 0.1 mM bromide (dotted line), or 1 mM chloride (dash-dotted line). (b) Dependence of the intensity of the first ECL peak (\square) and the second ECL peak (\circ) at a gold electrode on the concentration of bromide in 1 μM $\text{Ru}(\text{bpy})_3^{2+}$, 100 mM TPrA, and 0.15 M phosphate buffer solution (pH 7.5). Potential scan rate, 0.1 V/s.

Figure 11a shows the dependence of ECL intensity of 1 nM $\text{Ru}(\text{bpy})_3^{2+}$ on the concentration of TPrA in PBS in the absence or presence of bromide (optimum concentration). In the absence of bromide, the ECL intensity increased proportionally with TPrA concentration, which was in agreement with a previous report.^{4b} In the presence of the optimum concentration of bromide, however, the ECL intensity increased rapidly first with the TPrA concentration up to 50 mM, and then the intensity leveled off.

Using the PBS containing 50 mM TPrA and 1 mM bromide, lower concentrations of $\text{Ru}(\text{bpy})_3^{2+}$ could be detected (Figure 11b). Compared to the 100 mM TPrA buffer solution, the increase of ECL intensity by the bromide effect was around 4–5-fold.

CONCLUSIONS

The direct oxidation of TPrA at an electrode plays an important role in the ECL process of the $\text{Ru}(\text{bpy})_3^{2+}$ /TPrA system at low concentrations ($\leq 1 \mu\text{M}$) of $\text{Ru}(\text{bpy})_3^{2+}$. At a GC electrode, the direct oxidation of TPrA begins at ~ 0.6 V vs SCE and exhibits a broad irreversible anodic peak. In 1 μM $\text{Ru}(\text{bpy})_3^{2+}$, two ECL waves were observed: one in the potential region more negative than 1.0 V and one more positive than 1.0 V vs SCE. The first ECL wave was induced mainly by the direct oxidation of TPrA,

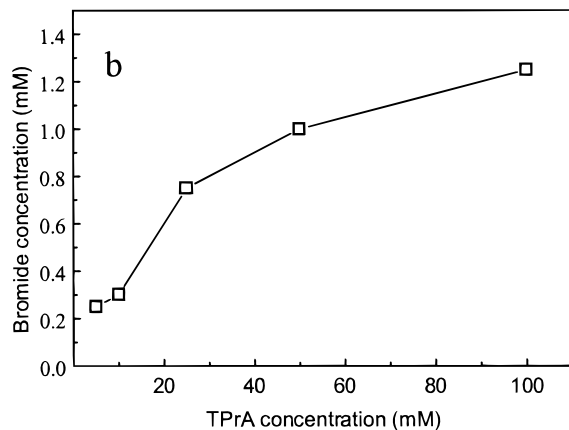
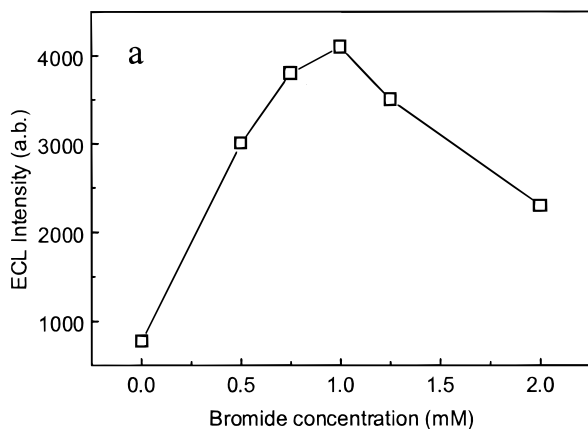


Figure 10. (a) Dependence of ECL intensity on bromide concentration in the flow-through system. Sample solution: 1 nM Ru(bpy)₃²⁺, 50 mM TPrA, 0.02 vol % Triton X-100, and 0.15 M phosphate buffer (pH 7.5). (b) Dependence of optimum concentration of bromide in the sample solution on TPrA concentration in the flow-through system. Sample solutions contained 1 nM Ru(bpy)₃²⁺ and 0.02 vol % Triton X-100. Background was subtracted from the signal.

and this result suggested lack of participation of Ru(bpy)₃³⁺ in the emission process. At Pt and Au electrodes, however, the direct oxidation of TPrA was inhibited significantly by the surface oxides formed during the anodic potential scan, and much weaker ECL is seen below 1.0 V. The main ECL peaks at these three types of electrodes all appeared at about 1.1–1.2 V. The large difference in ECL intensity at the different electrodes can be attributed to the importance of the direct oxidation of TPrA on the ECL processes and the effect of the nature of the electrode surface on this oxidation.

Based on the above results, an increase in the ECL intensity could be effected by promoting TPrA oxidation. At Pt and Au electrodes, a significant effect of addition of Br⁻ and I⁻ on TPrA oxidation was observed. The adsorption of halide species competed with the growth of surface oxides and significantly postponed the passivation of the electrode surface, resulting in a strong increase in the TPrA oxidation current. The anodic dissolution of gold in halide-containing solutions also played an important role in activating the gold electrode surface. An electrochemical catalytic effect of bromide oxidation to bromine also promoted the oxidation of TPrA. This halide effect on ECL at Pt and Au electrodes was significant with the most effective enhancement of ECL observed at a Au electrode by addition of bromide.

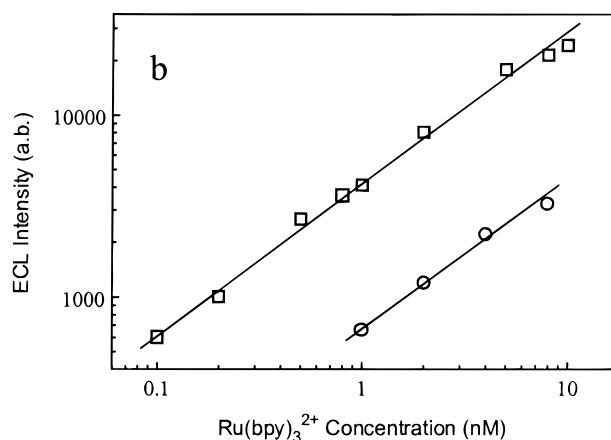
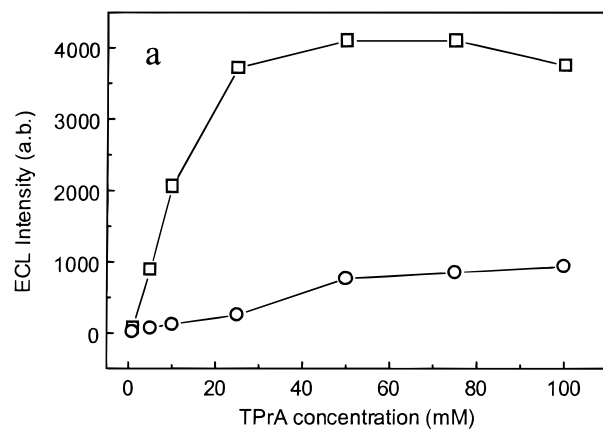


Figure 11. (a) Dependence of ECL intensity on TPrA concentration in the flow-through system. Sample solutions contained 1 nM Ru(bpy)₃²⁺ and 0.02 vol % Triton X-100 in the absence (○) or the presence of an optimum concentration of bromide (□) (see Figure 10b). (b) Dependence of ECL intensity on Ru(bpy)₃²⁺ concentration in the flow-through system. Sample solutions are 100 mM TPrA, 0.02 vol % Triton X-100, and 0.15 M phosphate buffer (pH 7.5) (○) or 1 mM bromide, 50 mM TPrA, 0.02 vol % Triton X-100, and 0.15 M phosphate buffer (pH 7.5) (□). Background was subtracted from the signal.

In the flow system, ECL intensity was also enhanced obviously by the addition of a small amount of bromide in the buffer solution. This provides a simple way of improving the detection sensitivity at low concentrations of Ru(bpy)₃²⁺.

ACKNOWLEDGMENT

The support of this research by IGEN, the National Science Foundation, the Robert A. Welch Foundation, and the Texas Advanced Research Program is gratefully acknowledged.

SUPPORTING INFORMATION AVAILABLE

Fluorescence spectra of aqueous Ru(bpy)₃²⁺ solutions containing various concentrations of iodine and bromine (PDF). This material is available free of charge via the Internet at <http://pubs.acs.org>.

Received for review February 22, 2000. Accepted April 26, 2000.

AC000199Y